

# Diffusion Characterization of Doped Oxide and Nitride Film

(도핑한 산화막 및 질화막의 확산특성)

李 鍾 德\*, 金 元 燦\*, 閔 弘 植\*, 李 晁 漢\*

(Jong Duk Lee, Won Chan Kim, Hong Shick Min and Chung Han Lee)

## 要 約

PECVD 방법으로 만들어진 도핑한 박막에서 실리콘으로의 인이나 붕소의 확산 특성이 연구되었다. CVD PSG 박막도 역시 만들어져 PECVD PSG에 있는 인의 확산특성과 나란히 비교되었다. 인의 확산은 N<sub>2</sub>와 O<sub>2</sub> 분위기 및 1,000°C, 1,050°C, 1,100°C의 온도에서 수행되었다. 붕소의 확산 변수들은 B<sub>2</sub>H<sub>6</sub> 유량 및 박막형성 온도를 달리하여 만들어진 박막에 관하여 고찰되었다. 실리콘으로의 주입물 확산 계수와 확산 Profile이 측정된 확산 깊이 및 불순물 표면 농도를 써서 Barry의 모델을 적용하여 계산되었다.

## Abstract

Phosphorus and boron diffusion from doped PECVD oxide films into silicon have been studied. CVD PSG was also prepared to parallely compare the diffusion characteristics of CVD PSG with that in PECVD PSG. The phosphorus diffusion experiments were performed in N<sub>2</sub> and O<sub>2</sub> ambient at the temperatures of 1000°C, 1050°C and 1100°C. The parameters of boron diffusion have been investigated from the doped film prepared by changing B<sub>2</sub>H<sub>6</sub> flow rate and deposition temperature. The diffusivities and diffusion profiles of the dopant into silicon were calculated by applying Barry's model using the measured parameters such as diffusion depth and surface concentration.

## I. Introduction

Standard diffusion techniques consist of a high temperature predeposition with a subsequent high temperature drive-in step. A short predeposition step is normally employed to saturate the surface with dopants. A drive-in

step without the presence of source is then used to redistribute the impurities and to achieve the final depth and surface concentration.

Diffusion sources are commonly deposited in essentially pure form, either as phosphorus oxide, or boron oxide and boron nitride[1] on the surface of the wafer. Before a final drive-in heat treatment, the oxide or the nitride layer is removed by etching, leaving a finite amount of the dopant in a shallow surface layer of the silicon prior to the deposition, or if the source layer is not uniform in composition, sheet resistivities across a wafer may vary significantly, and results from run-to-run will

\*正會員, 서울대학교 工科大学 電子工學科  
(Dept. of Electronics Eng., Seoul National Univ.)  
接受日字: 1984年 10月 27日  
(本 論文은 韓國學術振興財團의 1983年度 研究費 支  
援으로 研究되었음.)

not be reproducible. As a result, device yield will be lowered.

Since surface concentration of the dopant approaches solid solubilities, crystalline defects, especially edge dislocations, may be introduced in large numbers. These, in turn, influence the diffusion coefficient of the dopant as well as minority carrier life time and mobility in the surface regions.

The fact that the redistribution is accomplished without the presence of a source changes the type of distribution from complementary error function to modified Gaussian type. Furthermore, the control of depth and surface concentration become interdependent. The process is thus less easily controlled.

Ambient control is necessary because oxide may be regrown during the drive-in and a portion of the original impurities introduced in the deposition step is being consumed in the oxide. Diffusion of the dopants into silicon from doped oxide or nitride which have been deposited at low temperature provides a means of overcoming some of these problems.

A lower temperature reaction would minimize diffusion of the dopants into silicon during the deposition step. The surface concentration is no longer solid solubility limited and exact profile shape can be controlled by a single environment annealing step. Surface concentration in silicon is nearly independent of the time of diffusion cycle since the oxide acts as almost constant reservoir for the dopant. Since surface concentrations in silicon are allowed below the silicon solubility, minimum number of dislocations are introduced during diffusion.

Furthermore, the surface film containing dopant can be sometimes retained throughout the processing of the device, simplifying the fabrication procedure and making the device less sensitive to contaminants present in the furnace during diffusion.[2]

Since the control of surface concentration is simplified, the electrical characteristics of device can be held in tighter tolerance. Ultimately, these advantages lead higher yields. These doped diffusion sources can be deposited by a variety of means, such as anodization, APCVD, LPCVD, PECVD or reactive sputtering.

In this paper, the diffusion of phosphorus

and boron into silicon from doped oxide layers deposited by PECVD has been studied. In CVD systems where the energy is supplied only thermally, the addition of large quantities of n-type dopant during deposition greatly decreases deposition rates.[3] In addition, differences in the decomposition rates of the silicon containing gas make uniformity control difficult. Using plasma to aid the decomposition of the reactant gases can be expected to remove some of limitations previously encountered.

## II. Theory

Barry and Olofsen have given a detailed mathematical description of a model for the evaluation of diffusion from a doped oxide layer with or without a finite oxide barrier of thickness  $x_B$ . [4,5,6] Fig. 1 shows a schematic representation of different layers together with diffusion parameters.

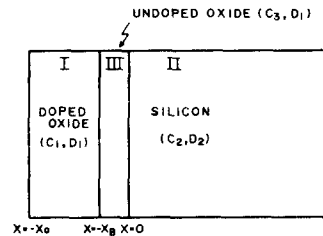


Fig. 1. Diffusion from a doped oxide through an undoped oxide of thickness  $x_B$  into semiconductor substrate.

They assumed that diffusion coefficient is not a function of concentration. They ignored the effect arising from field-aided diffusion of ionized dopants. The expected impurity distribution after diffusion from semi-infinite source layer without finite oxide barrier is

$$C_2 = C_s \operatorname{erfc} (x/2\sqrt{D_2 t}) \quad (1)$$

and

$$C_s = C_o \sqrt{D_1/D_2} / (1+m^{-1} \sqrt{D_1/D_2}) \quad (2)$$

where  $C_o$  is the initial concentration of the dopant in the oxide,  $D_1$  and  $D_2$  are diffusivities

of the dopant in the oxide and semiconductor, respectively. Segregation coefficient  $m$  is defined by the equation,  $m=C_2(0,t)/C_1(0,t)$ .

We find that the surface concentration becomes time invariant from equation (2). If the substrate is silicon with resistivity of about 2 ohm-cm of opposite type from the diffusing dopant, equation (1) and (2) can be manipulated to yield

$$x_j = 2\sqrt{D_2 t} \cdot \arg [\operatorname{erfc}(C_b/C_s)] \quad (3)$$

and

$$\begin{aligned} I/V &= 8.15 \times 10^{-23} \bar{\mu} C_s \sqrt{D_2 t} \\ &= 8.15 \times 10^{-23} \bar{\mu} C_o (1+m^{-1} \sqrt{D_1/D_2})^{-1} \\ &\quad \sqrt{D_1 t} \end{aligned} \quad (4)$$

where  $\mu$  is the effective mean mobility of carriers,  $x_j$  is the junction depth, and  $I/V$  is the sheet resistivity measured with a standard four-point probe.  $C_b$  is the bulk concentration of carriers in the substrate.

Equation (3) and (4) represent that junction depth and sheet conductivity are linear functions of square root of diffusion time. If we measure the surface concentration of the dopants, it is possible to determine  $D_2$  from junction depth and sheet resistivity data.

The most important consequences of this model for the concentration profile in silicon are time invariant surface concentration and well known complementary error function profile. Similar doping profile depending on diffusion length in the oxide was obtained by Owen and Schmidt.[7] However, serious deviations in Barry's model occur at high surface concentrations. The reason for these deviations is not exactly known at the present time, but some people proposed several hypotheses such as nonequilibrium at the oxide-silicon interface, concentration dependence of the diffusivity of the dopant in the oxide, and so forth. [8,9]

In comparison with Barry's model which focused on segregation phenomena, R.N. Ghostagore proposed a phenomenological model which based on lower dopant diffusivity in the oxide phase and chemical transformation at the oxide-silicon interface.[10]

He introduced new parameters like surface barrier constants in place of segregation coefficient and derived the expression for time-varying surface concentration and total amount of dopants per unit area.[10]

### III. Experimental

P-doped oxides for diffusion experiments were deposited by ASM PECVD system. The wafers are held adjacent to closely spaced vertical electrodes. RF (13.56 MHz) power is supplied to each set and entire electrode assembly is contained in the evacuated chamber within a resistant-heated furnace. ANELVA PD-301 was used to deposit B-doped oxides. PD-301 is a capacitive type of plasma reactor. Substrate heating is achieved by attaching heating plate and water cooling device under the electrode.

The silicon substrates used for PSG and BSG were 6-9 ohm-cm p-type and 3-4 ohm-cm n-type silicon wafers respectively. All the substrates were (100) surface-oriented wafers with 4-inch diameter.

The conditions for deposition experiments were listed in Table I. The reactant gases used for p-doped oxide deposition were high purity  $\text{SiH}_4$ ,  $\text{O}_2$  and 5%  $\text{PH}_3$  in  $\text{N}_2$ . The carrier gas was highly pure  $\text{N}_2\text{O}$ . B-doped oxides were deposited using  $\text{SiH}_4$ ,  $\text{N}_2\text{O}$  and 1%  $\text{B}_2\text{H}_6$  in  $\text{H}_2$ . We also tried to prepare BN film using 1%  $\text{B}_2\text{H}_6$  in  $\text{H}_2$ ,  $\text{NH}_3$  and  $\text{N}_2$ , but it was hardly formed. 1% diborane was too diluted in  $\text{H}_2$  to form BN film. Spectral analysis of the 1%  $\text{B}_2\text{H}_6$  plasma showed no trace of boron implying the two spectra obtained from  $\text{H}_2$  and 1%  $\text{B}_2\text{H}_6$  in  $\text{N}_2$  were identical. W. Schmolla, *et al* reported a-BN film formation from PECVD using organic compounds ( $\text{BH}_3$ ,  $\text{HN}(\text{CH}_3)_2$  and  $\text{BH}_3\text{N}(\text{C}_2\text{H}_5)_3$ ) for boron, and  $\text{NH}_3$  and  $\text{N}_2$  for nitrogen.[11]

The compositions of PSG can be determined by FTIR spectra and XRF analysis.[12] Refractive index and thickness of as deposited films were measured by an ellipsometer and a spectrophotometer. P-doped oxides had the refractive index of 1.543 and the thickness of about 7000 Å. The refractive index of BSG varied from 1.430 to 1.668 as deposition

Table 1 . The preparation conditions for PECVD PSG and BSG

equipment	P1	P2	P3	P4	P5	P6	B1	B2	B3	B4	B5	B6
equipment	ASM						PD-301					
pressure (torr)	0.78						0.4					
power (watt)	150						20					
temperature ( °C )	380						265	260	250	100	200	380
time (minute)	14						1.5					
SiH4 (sccm)	78						10					
N20 (sccm)	1500						48					
O2 (sccm)	14						—					
PH3 (sccm)	3	10	13	17	21	39						
B2H6 (sccm)							4	7	10	10	10	10
thickness (Å) °	6200	7200	7000	7000	6500	7200	938	961	930	1278	973	648
refractive index	1.543						1.447	1.478	1.493	1.430	1.471	1.618

temperature increased for the film thickness of 1000 Å. The 1000 Å B-doped films were covered with 4000 Å pure oxide to prevent out-diffusion and furnace contamination during diffusion.

Diffusion experiments were performed in conventional horizontal diffusion furnace consisting of electrically heated fused quartz tube. The junction depth of n-type and p-type layers were determined by staining n-type area after angle lapping and grooving. Surface concentration and doping profiles were determined using anodization-sectioning in conjunction with the four-point probe differential sheet resistivities. Anodization was performed using a solution of 0.04N KNO<sub>3</sub> in ethylene glycol 100 cc.<sup>[13]</sup> The oxide thickness resulting from one anodization was 950±30 Å and the refractive index of anodic oxide was 1.47. Doping profiles were calculated by Donovan and Evans' conversion method.<sup>[14]</sup>

After diffusion, the surface of PSG layers were investigated by microscope and SEM. The presence of craters and clusters was observed in various degrees depending upon doping concentrations and annealing conditions. It was estimated that the diameters of these defects were often several times larger than film thickness. These defects in phosphorus doped oxide films are supposed to be small crystallites formed at localized nucleation centers, such as impurities and contaminants during heat treatment.

CVD PSG made by pyrolytic decomposition was prepared to compare with PECVD

PSG in this experiment. Phosphorus concentration was 4 m/o estimated using A.S. Tenney and M. Ghezzi's calibration curve of linear absorbance ratio vs. P<sub>2</sub>O<sub>5</sub> m/o.<sup>[15]</sup>

#### IV. Results and Discussion

The FTIR spectra of various PSG films are shown in Fig. 2. Hydrogen-containing bonds are Si-OH at 885 cm<sup>-1</sup> and 940 cm<sup>-1</sup>, and Si-H at 630 cm<sup>-1</sup> and 805 cm<sup>-1</sup>.<sup>[16]</sup> The peaks at 450 cm<sup>-1</sup>, 805 cm<sup>-1</sup> and 1070 cm<sup>-1</sup> represent

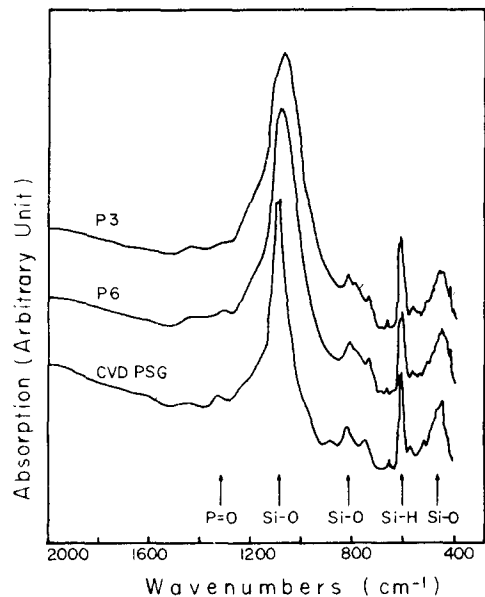


Fig. 2. FTIR spectra of PSG films with various compositions.

Si-O bonds and the peak at  $1325\text{ cm}^{-1}$  stands for P=O bond. P=O bond in PECVD PSG grows depending on  $\text{PH}_3/\text{SiH}_4$  ratio, but the peak development of P=O bond in PECVD PSG does not increase as much as expected in CVD PSG.

The uniformity and the reproducibility in run-to-run and day-to-day of a phosphorus diffusion layer in silicon become important when P-doped oxide is used as a diffusion source. To obtain the distribution of diffusion layer when phosphorus diffused into 6-9 ohm-cm p-type silicon at  $1100^\circ\text{C}$  in a dry  $\text{N}_2$  ambient for 2 hours, a conventional four-point probe was moved from one point to the next point with an interval of 5 mm over the entire surface of Si wafer. The reproducibility of sheet resistivity from day-to-day is about  $\pm 5\%$ . Across a wafer its maximum variation is about  $\pm 3\%$ . This result is satisfactory when it compared with about  $\pm 10\%$  of sheet resistivity distribution obtained from CVD PSG diffusion layer.

After diffusing for 20 minutes at  $1100^\circ\text{C}$  and in  $\text{N}_2$  with 1%  $\text{O}_2$ , surface concentration  $C_s$  and sheet resistivity  $R_s$  are in Fig. 3 as a function of  $\text{PH}_3/\text{SiH}_4$ . Saturation effects are observed for both parameters.

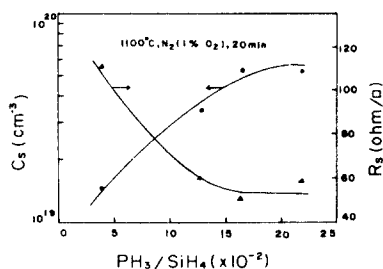


Fig. 3. Sheet resistivity  $R_s$  and surface concentration  $C_s$  depending on  $\text{PH}_3/\text{SiH}_4$  ratio after diffusion.

The junction depth  $x_j$  and sheet conductivity  $R_s^{-1}$  are of importance in the characterization of diffused layer in the semiconductor technology. These parameters are plotted in Fig. 4 and 5 for two diffusion temperatures of  $1100^\circ\text{C}$  and  $1000^\circ\text{C}$ , and for the glasses with composition of 1.2 m/o and 6.5 m/o  $\text{P}_2\text{O}_5$ . Linearity is obtained in  $x_j$  and  $R_s^{-1}$  plots as we know from equation (3) and (4).

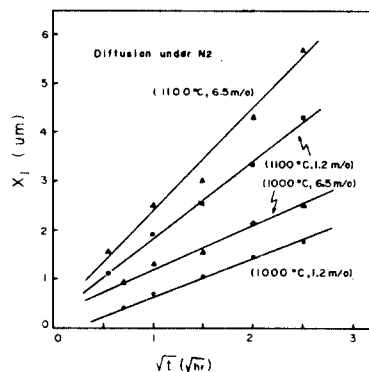


Fig. 4. Junction depth  $x_j$  depending on square root diffusion time, diffusion temperature and PSG composition.

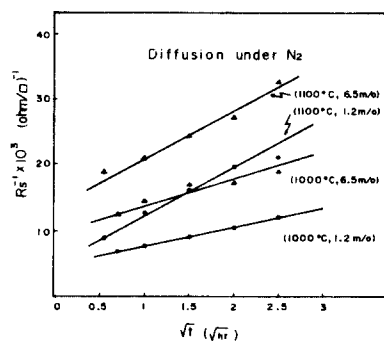


Fig. 5. Sheet conductivity  $R_s^{-1}$  versus square root of diffusion time resulting from phosphorus diffusion in  $\text{N}_2$ .

To compare diffusion characteristics of CVD PSG with those of PECVD PSG,  $x_j$  and  $R_s^{-1}$  are plotted as a function of square root of diffusion time in Fig. 6 and 7.

Those  $x_j$  and  $R_s^{-1}$  of CVD PSG are larger than those extracted from PECVD PSG. Surface concentrations of layers diffused at  $1050^\circ\text{C}$  and in  $\text{N}_2$  from PECVD with composition of 1.2 m/o and 6.5 m/o  $\text{P}_2\text{O}_5$  correspond to those of the diffused layers from CVD PSG with composition of 1.1 m/o and 1.8 m/o  $\text{P}_2\text{O}_5$  respectively. We calculated  $D_2$  and  $C_s$  using the measured  $x_j$  and  $R_s$ , and borrowing the phosphorus diffusivity in oxide,[5] and listed the results in Table II. In Fig. 8,  $C_s$  is not constant depending on diffusion time. However,  $D_2$  is proportional to  $[\text{arg}(\text{erfc}(C_b/C_s))]^{-2}$

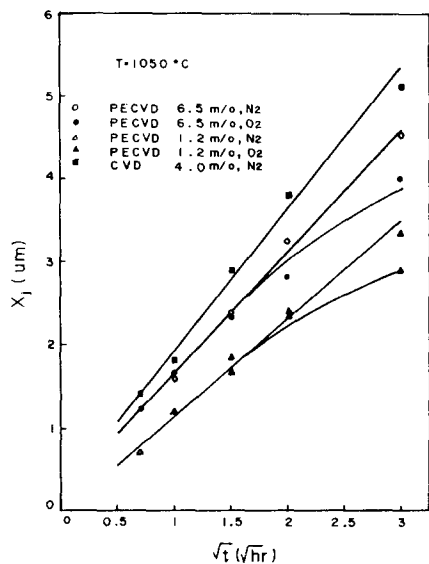


Fig. 6. Junction depth  $x_j$  depending on square root of diffusion time for the diffusion from PECVD and CVD phosphorus doped oxides in  $N_2$  and  $O_2$ .

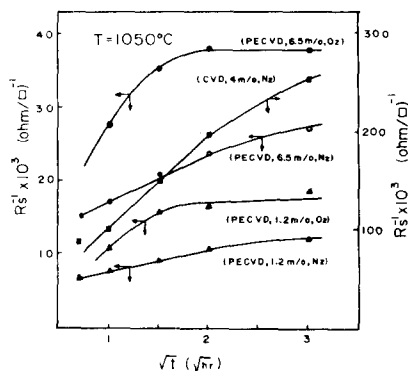


Fig. 7. Sheet conductivity vs. square root of diffusion time for the diffusion from PECVD and CVD oxides in  $O_2$  and  $N_2$ .

and  $X_j^2$  as shown in equation (2) and (3) respectively. We take  $C_s$  as constant because it is weakly dependent on  $D_2$  and because it does not change significantly (less than 8% in log scale). PECVD with 6.5 m/o and CVD with 1.8 m/o may show the same results after diffusion at  $1050^\circ\text{C}$ . The reason is that more excess dopants can come to the glass during normal CVD than PECVD process. That

means plasma ions are more active than the thermally activated atoms to form P=O bond so that there is less chance to be excess dopants in the process of plasma deposition.

For the diffusion condition of high temperature ( $\geq 1100^\circ\text{C}$ ) and high concentration ( $> 6.5$  m/o) source layer, many craters and clusters are appeared on the PECVD film after diffusion while no defects are observed on the CVD film of 4 m/o.

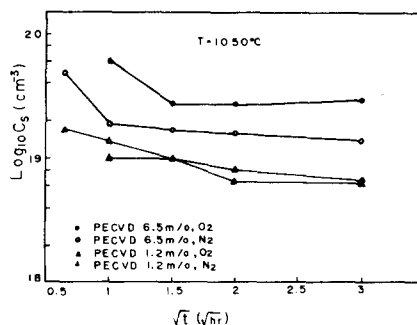
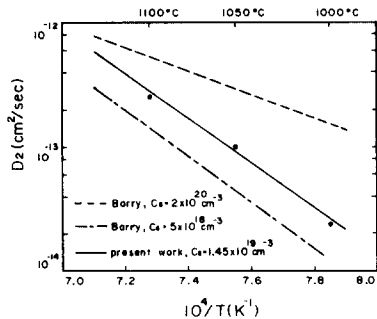


Fig. 8. Surface concentration vs. square root of diffusion time for the diffusion from PECVD PSG in silicon.

The results of  $x_j$ ,  $R_s^{-1}$ , and  $C_s$  depending on  $\sqrt{t}$  in  $O_2$  ambient are also plotted in Fig. 6, 7, and 8. When the diffusion was done for more than 2 hours, junction depths observed from the diffusion in  $O_2$  become smaller than the values found in  $N_2$  as shown in Fig. 6. This effect can be explained by the fact that an undoped oxide layer grows between the deposited layer of doped oxide and the silicon substrate in  $O_2$  ambient and acts as a diffusion barrier. By diffusion after a certain time in  $O_2$  ambient the sheet conductivity  $R_s^{-1}$  remains almost constant. This is because the growth of undoped barrier stops further diffusion from the source into silicon. Higher sheet conductivity and surface concentration are obtained in the presence of  $O_2$  when compared with those of identical wafers diffused in an inert atmosphere of  $N_2$  under the same diffusion condition. If ionic oxygens are present likely in the process of thermal oxidation of silicon, [17] the impurity in PSG in the vicinity of the oxide-silicon interface can be field-aided. Thus, an enhanced impurity diffusion

at this interface can give rise to higher surface concentration and sheet conductivity.



**Fig. 9** Phosphorus diffusivity depending on diffusion temperature.  $C_S=1.45 \times 10^{19} \text{ cm}^{-3}$  for the present work is the measured value after  $1050^\circ\text{C}$  diffusion.

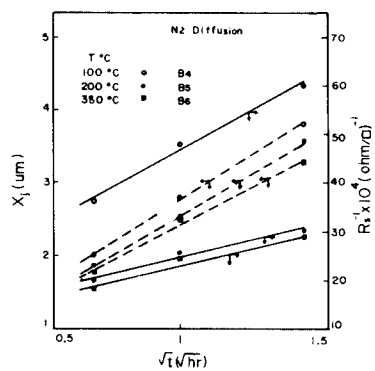
The results for  $D_2$  obtained in this experiment concerning the temperature dependence of  $x_j$  and  $C_S$  are shown in Fig. 9 and summarized in Table II. Barry modelled time-invariant surface concentration and confirmed it by measuring  $C_O$  and  $C_S$  independently. However, we find that  $C_S$  decreases as temperature and/or time increase with constant  $C_O$  as shown in Fig. 8 and Table II. These results suggest that doped oxide can not act as a constant reservoir and  $D_2$  increases faster than  $D_1$  with temperature rise as understood from equation (2). The diffusivity was calculated from the slope of the plot,  $x_j$  vs.  $\sqrt{t}$  and the measured surface concentration. An activation energy of 3.4 eV for the surface concentration of  $1.45 \times 10^{19} \text{ cm}^{-3}$  was extract-

Table 2. The calculated  $D_2$  from the measured parameters  $C_s$  and  $x_j$  using equation (3) after diffusion at various temperature under  $N_2$

	PECVD 1.2m/o PSG		PECVD 6.5m/o PSG	
T ( C )	$C_s(\text{cm}^{-3})$	$D_2(\mu\text{m}^2/\text{hr})$	$C_s(\text{cm}^{-3})$	$D_2(\mu\text{m}^2/\text{hr})$
1000	$1.50 \times 10^{19}$	0.020	$2.4 \times 10^{19}$	0.023
1050	$1.45 \times 10^{19}$	0.040	$1.8 \times 10^{19}$	0.063
1100	$6.32 \times 10^{18}$	0.090	$1.7 \times 10^{19}$	0.116

ed from the slope of the curve  $\ln D_2$  vs.  $T^{-1}$  and compared with those of 2.6 eV and 3.7 eV for the surface concentration  $2 \times 10^{20} \text{ cm}^{-3}$  and  $5 \times 10^{18} \text{ cm}^{-3}$  estimated by Barry.[5] The boron diffusivity in silicon was  $0.36 \mu\text{m}^2/\text{hr}$  for the diffusion conditions of  $1200^\circ\text{C}$  and  $N_2$  atmosphere.

BSG diffusion experiments were also performed at  $1200^\circ\text{C}$  in  $N_2$  ambient.  $x_j$  and  $R_S^{-1}$  are plotted depending on deposition temperature and diffusion time in Fig. 10.  $x_j$  and  $R_S^{-1}$  are linear functions of  $\sqrt{t}$  and decrease with rise in deposition temperature.



**Fig. 10** Junction depth  $x_j$  and sheet conductivity  $R_S^{-1}$  resulting from diffusion of boron into silicon at  $1200^\circ\text{C}$ .

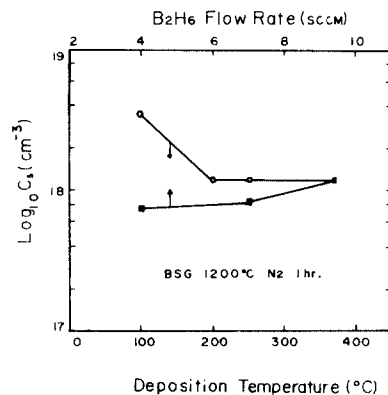


**Fig. 11** And in  $N_2$  ambient for the samples of  $B_4$ ,  $B_5$  and  $B_6$  surface concentration depending on deposition temperature and  $B_2H_6$  flow rate after diffusion of BSG

The surface concentration of the diffused layer for 60 minutes in  $N_2$  ambient is shown in Fig. 11. Surface concentrations increase with  $B_2H_6$  flow rates from  $7.4 \times 10^{17} \text{ cm}^{-3}$  to  $2 \times 10^{18} \text{ cm}^{-3}$ . Saturation of  $C_s$  occurs at the deposition temperature of about  $200^\circ\text{C}$ .

Doping profiles of n-type and p-type layers together with complementary error function using the experimentally obtained diffusivity are plotted in Fig. 12 and 13 respectively. Both of doping profiles were almost the same as complementary error function except near

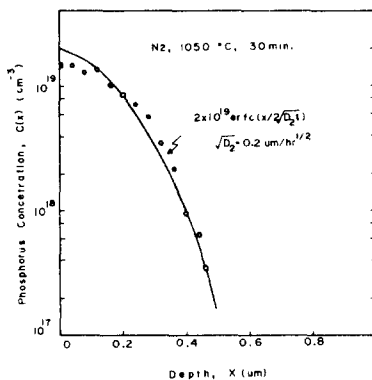


Fig. 12 Comparison of theoretical curve with actual doping profile. PSG film with a composition of 1.2 m/o was used for diffusion experiment at  $1050^\circ\text{C}$ , for 30 minutes and in  $N_2$  ambient.

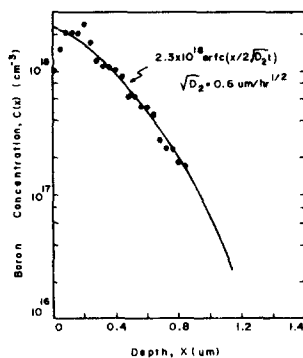


Fig. 13 Comparison of an erfc distribution with an actual doping profile. BSG film deposited with flow rate ratio of  $B_2H_6$  to  $SiH_4$  0.01 was used for diffusion at  $1200^\circ\text{C}$ , for 30 minutes and in  $N_2$  ambient.

the surface region. Fig. 13 shows that boron was depleted at the surface region because boron diffusivity in oxide is relatively large.

## V. Conclusions

Diffusions of boron and phosphorus from PECVD doped oxide sources were investigated. Considering the lower diffusion parameters and the insignificant development of P=O bond of PSG, PECVD gives much more stoichiometric reaction than normal pressure CVD. The diffusion of phosphorus was enhanced in the presence of  $O_2$  to yield higher surface concentration and higher sheet conductivity. Doping profiles of diffused layer were almost complementary error function except near the surface region, while boron was depleted at the surface region. Maximum surface concentration of diffused layers from BSG and PSG shows about an order of  $10^{19} \text{ cm}^{-3}$  which can be used for base diffusion, CMOS n- and p-well formation during IC fabrication. However, high concentration diffusion which is needed for emitter junction and source/drain diffusion can not be achieved by using doped PECVD sources. It is necessary to study more with high concentration  $B_2H_6$  gas than 1% to obtain high concentration ( $>10^{18} \text{ cm}^{-3}$ ) BSG as well as PECVD boron nitride films with excess boron.

## References

- [1] Katsufusa Shohno, Tejin Kim, and Chol Kim, *J. of Electrochem. Soc.*, vol. 127, no. 7, pp. 1546-1550, July 1980.
- [2] J. Scott and J. Olmstead, *RCA Review*, vol. 26, pp. 357-368, September 1965.
- [3] F. C. Eversteyn and B. H. Put, *J of Electrochem. Soc.*, vol. 120, pp. 106, 1973.
- [4] M. L. Barry and P. Olofsen, *ibid*, vol. 116, no. 6, pp. 854-860, June 1969.
- [5] M. L. Barry, *ibid*, vol. 117, no. 11, pp. 1406-1410, Nov. 1970.
- [6] M. L. Barry and J. Manoliu, *ibid*, vol. 117, no. 2, pp. 854-860, Feb. 1970.
- [7] A. E. Owen and P. F. Schmidt, *ibid*, vol. 115, no. 5, pp. 548-553, May 1968.



- [8] P. J. Gielisse, T. J. Rockett, and W. R. Foster, Ohio State University Research Foundation, Report 931, 1961.
- [9] R. B. Fair, *J. of Electrochem. Soc.*, vol. 122, P. 800, 1975.
- [10] R. N. Ghostagore, *Solid-State Electronics*, vol. 17, pp. 1065-1073, 1974.
- [11] W. Schmolla and H. L. Hartnagel, *ibid*, vol. 126, no. 10, pp. 2326-2335, Oct. 1982.
- [12] Hyun Gyu Yoo, *Private Communication*. KIET' Aug. 1984.
- [13] E. F. Duffek, E. A. Benjamin, and C. Myloic, *Electrochem. Technology*, vol. 3, no. 3-4, pp. 75-80, Mar.-Apr. 1965.
- [14] R. A. Evans and R. P. Donovan, *Solid-State Electronics*, vol. 10, pp. 155-157, 1967.
- [15] A. S. Tenny and M. Ghezzeo, *J. Electrochem. Soc.*, vol. 120, no. 9, pp. 1276-1279, Sept. 1973.
- [16] P. J. Jorgensen, *J. Chem. Phys.*, vol. 37, no. 4, pp. 874-877, 1962.
- [17] A. C. Adams, *Solid State Technology*, pp 135-139, April, 1983.
-